Biochemical and Biophysical Research Communications 450 (2014) 500–506

Contents lists available at ScienceDirect

Biochemical and Biophysical Research Communications

journal homepage: www.elsevier.com/locate/ybbrc

Mitofusin 2 decreases intracellular lipids in macrophages by regulating peroxisome proliferator-activated receptor-γ

Chun Liu [a], Beihai Ge [a], Chao He [b], Yi Zhang [a], Xiaowen Liu [a], Kejian Liu [c], Cuiping Qian [a], Yu Zhang [a], Wenzhong Peng [a], Xiaomei Guo [a,*]

[a] Department of Cardiology, Tongji Hospital, Tongji Medical College, Huazhong University of Science and Technology, 1095 Jiefang Avenue, Wuhan 430030, PR China
[b] Department of Cardiology, China Three Gorges University, Yichang 433000, PR China
[c] Department of Cardiology, The First Affiliated Hospital of Medical College, Shihezi University, PR China

ARTICLE INFO

Article history:
Received 28 May 2014
Available online 10 June 2014

Keywords:
Mitofusin 2
ATP binding cassette transporter A1
ATP binding cassette transporter G1
Scavenger receptor class B type I
Peroxisome proliferator-activated receptor γ

ABSTRACT

Mitofusin 2 (Mfn2) inhibits atherosclerotic plaque formation, but the underlying mechanism remains elusive. This study aims to reveal how Mfn2 functions in the atherosclerosis. Mfn2 expression was found to be significantly reduced in arterial atherosclerotic lesions of both mice and human compared with healthy counterparts. Here, we observed that Mfn2 increased cellular cholesterol transporter expression in macrophages by upregulating peroxisome proliferator-activated receptor-γ, an effect achieved at least partially by inhibiting extracellular signal-regulated kinase1/2 (ERK1/2) and p38 mitogen-activated protein kinases (MAPKs) pathway. These findings provide insights into potential mechanisms of Mfn2-mediated alterations in cholesterol transporter expression, which may have significant implications for the treatment of atherosclerotic heart disease.

1. Introduction

Atherosclerotic heart disease, is a leading cause of global morbidity and mortality with its incidence continuously increasing worldwide. It is caused by atherosclerosis plaque formation, a complicated inflammatory process in which almost all cell types associated with the arterial wall are involved, including macrophages, smooth muscle cells and endothelial cells [1]. Macrophages play an important role in both lipid metabolism and inflammation and are central to the pathogenesis of atherosclerosis [1]. Thus, regulation of lipid metabolism and inflammation by macrophages is a target for the treatment of atherosclerotic diseases [1].

The expression of target genes of lipid homeostasis and glucose metabolism, together with inflammation involved in atherosclerosis, are regulated by a ligand-activated transcription factor of the nuclear receptor superfamily-peroxisome proliferator-activated receptor-γ (PPARγ) [2,3]. PPARγ can be phosphorylated and inactivated by the ERK/MAPKs and p38/MAPKs signaling pathway [4,5]. The activation of PPARγ induces the expression of the cholesterol efflux protein ABCA1 in macrophages and suppresses the progression of atherosclerosis in apoE knockout mice, thus exerting protective effects against atherosclerosis [6].

The mitochondrial outer membrane protein Mfn2 is pivotal in regulating mitochondrial fusion, maintaining mitochondrial morphology and homeostasis. As important sources and targets of reactive oxygen species (ROS), mitochondria are crucially involved in atherogenesis [7]. Mfn2, recognized as an endogenous Ras inhibitor, regulates cell proliferation and apoptosis, oxidative stress, autophagy, glucose and lipid homeostasis involved in atherosclerosis [7,8]. Mfn2 expression is reduced in the muscle of people with obesity or type 2 diabetes compared to people without these conditions [9]. Mitochondrial dysfunction reduces the efficiency of the cholesterol efflux pathway in RAW264.7 cells, leading to regression and stabilization of atherosclerotic plaques [10,11]. In addition, Mfn2 expression is downregulated in mice fed with a high fat diet (HFD), and overexpression of Mfn2 alleviates HFD-induced hepatic steatosis [12]. These results suggest that Mfn2 is involved in the pathophysiology of metabolic diseases such as atherosclerosis. However, the mechanisms of how Mfn2 contribute to atherosclerosis, especially cholesterol transport, are poorly understood. In this study, we aimed to investigate whether Mfn2 was involved in lipid metabolism of foam cell formation through the regulation of cholesterol transport.

* Corresponding author. Fax: +86 27 83646605.
E-mail addresses: xmguo@tjh.tjmu.edu.cn, liuchuntongji@163.com (X. Guo).

http://dx.doi.org/10.1016/j.bbrc.2014.06.005
0006-291X/

2. Materials and methods

2.1. Cell culture and treatment

Human THP-1 monocytes (from American Type Culture Collection, USA) were grown in RPMI-1640 medium supplemented with 10% fetal bovine serum, 2 mM L-glutamine, 100 U/mL of penicillin and 100 μg/mL of streptomycin (Gibico, USA) at 37 °C in a humid atmosphere with 5% CO_2. THP-1 monocytes were differentiated into macrophage-like cells by pre-incubation with 320 nM PMA for 24 h, then infected by adv-lacZ, adv-Mfn2 or adv-siRNA (recombinant Mfn2 siRNA adenovirus) for 24 h as described previously [13]. Next the cells were treated with indicated doses of rosiglitazone, GW9662, PD98059 and SB203580.

2.2. Quantitative real-time polymerase chain reaction (PCR)

Total RNA was isolated using TRIzol reagent (Invitrogen) and cDNA synthesis was performed with a RevertAid First Strand cDNA synthesis kit (Fermentas) according to the manufacturer's instructions. Quantitative real-time PCR was performed on a LightCycler 480II (Roche) using the SYBR green polymerase chain reaction master kit (TOYOBO). The absolute number of copies of the gene of interest was calculated from the linear regression of a standard curve. The primer sequences for ABCA1, ABCG1, SR-BI, LXRα, PPARγ and Mfn2 were listed in Table 1. The expression of the measured genes was normalized to GAPDH.

2.3. Immunofluorescence and immunohistochemistry

Cardiovascular segments and cell climbing films were fixed in 4% formalin and embedded in paraffin. Serial 5 μm specimens were cut and stained with hematoxylin-eosin. In addition, the specimens were blocked with phosphate-buffered saline (PBS) containing 4% BSA for 30 min at room temperature, and then incubated with primary antibodies for Mfn2, CD68 and SR-A at 4 °C overnight. For immunofluorescence analysis, the specimens were incubated with secondary antibody conjugated with FITC. For immunohistochemistry analysis, the specimens were incubated with horseradish peroxidase-conjugated secondary antibody and visualized with 3,3′-diaminobenzidine. The specimens were observed under a two-photon laser scanning confocal microscope (NOL-LSM 710, Carl Zeiss) and images were analyzed with software ImagePro-Plus 6.0.

2.4. Statistical analysis

Data were expressed as mean ± SD and analyzed by GraphPad Prism 5 software. Significant differences were determined using a two-tailed unpaired Student's t test. $p < 0.05$ was accepted as statistically significant.

Materials, animals and clinical subjects, recombinant adenoviruses preparation and infection, preparation of oxLDL, oil red O staining, cellular cholesterol analysis and western blot analysis are described in the Supplemental information.

Table 1
Sequence of primers used to quantify mRNA by PCR.

Gene	Forward primer	Reverse primer
ABCA1	TCTCACCACTTCGGTCTCCAT	ACAGCCACCTTCATCCCATCT
ABCG1	GCCAGGAAACAGGAAGATTAGAC	GAGACACCCACAAACCCAACG
SR-BI	GGCGGTGATGATGGAGAATAA	AGAGCCCAGAGTCGGAGTTGT
LXRα	TTTGCCTTGCTCATTGCTATCAG	ATTAGCATCCGTGGGAACATCAG
PPARγ	CCATTCACCCCGCTTTTGACTAT	GCTTTTTACATACTTCACCTTTGG
Mfn2	GGCTCAAGACTATAAGCTGCGAA	GGAGGGGTTTCAAGCCATCTAT
GAPDH	GGTCGGAGTCAACGGATTTG	GGAAGATGGTGATGGGATTTC

3. Results

3.1. Mfn2 expression in atherosclerotic lesions in mouse and human arteries

To assess the relationship between Mfn2 and atherosclerosis, we first analyzed the aortas of apoE−/− mice and C57/BL mice fed with a HFD diet for 12 weeks. Atherosclerotic lesions increased in apoE−/− mice compared with C57BL/6 mice (Fig. 1A and B below), and Mfn2 protein in the aortas was detected by Western blot analysis (Fig. 1B above) and immunostaining (Fig. 1C). Images of mouse aortas showed that Mfn2 presents a lower expression in atherosclerotic apoE−/− mice arteries than in nonatherosclerotic C57/BL mice arteries (Fig. 1C).

To reveal the correlation between Mfn2 expression and macrophage-derived foam cells in atherosclerotic lesions, we located Mfn2 and macrophages in human atherosclerotic arteries by using antibodies against Mfn2 and CD68. CD68-positive macrophages were abundant in human atherosclerosis plaques, but only slightly detectable in normal arteries. Meanwhile, Mfn2 protein was marginally detectable in the atherosclerotic plaques of CHD patients compared to nonatherosclerotic coronary arteries and aortas in healthy volunteers (Fig. 1D). Furthermore, Mfn2 protein and mRNA levels were significantly downregulated in atherosclerotic arterial lesions of human coronary arteries compared to their normal counterparts (Fig. 1E).

Moreover, cultured THP-1 cells treated by oxLDL showed significantly less Mfn2 expression than cells cultured with PBS alone or LDL alone (Fig. 1F), in a dose-dependent way (Fig. S1.A).

3.2. Mfn2 decreases cellular cholesterol content in macrophages

To evaluate the effect of Mfn2 on cellular cholesterol levels, we extracted lipids from THP-1 cells treated with PBS (con), oxLDL + vector control (adv-lacZ), oxLDL + 60 pfu adv-Mfn2 (adv-Mfn2-60), oxLDL + 60 pfu adv-siRNA (adv-siRNA-60), and measured total and free cellular cholesterol content. The optimal conditions for adenovirus vector infection of THP-1 macrophages were determined to be at a titer of 40 or 60 pfu, with most cells expressing GFP without obvious cytotoxicity (data not shown, images of adv-siRNA infection efficiency are shown in Supplemental Fig. S1.B). Western blot analysis confirmed that Mfn2 expression was significantly increased in cells infected by adv-Mfn2 and decreased in those infected by adv-siRNA, respectively, compared with vector controls ($p < 0.01$; Fig. 2A and B).

Oil red O staining showed that Mfn2 decreased lipid accumulation in macrophages only in the presence oxLDL (80 μg/mL, 24 h) (Fig. 2C). Adv-siRNA had no significant effect on cellular free cholesterol levels, but increased total cholesterol and cholesterol ester ratio. Mfn2 overexpression (adv-Mfn2-60) significantly decreased total cholesterol level and cholesterol ester ratio, compared with oxLDL + empty vector control (adv-lacZ) (Fig. 2D). These data suggested that Mfn2 decreases cellular cholesterol level in THP-1 macrophages.

3.3. Mfn2 regulates the expression of cholesterol transport proteins and PPARγ in macrophages

To understand how Mfn2 regulates cellular cholesterol level in macrophages, we investigated the effects of Mfn2 on cholesterol transport proteins such as ABCA1, ABCG1, SR-BI and SR-A in THP-1 macrophages. Adv-Mfn2 mediated overexpression of Mfn2

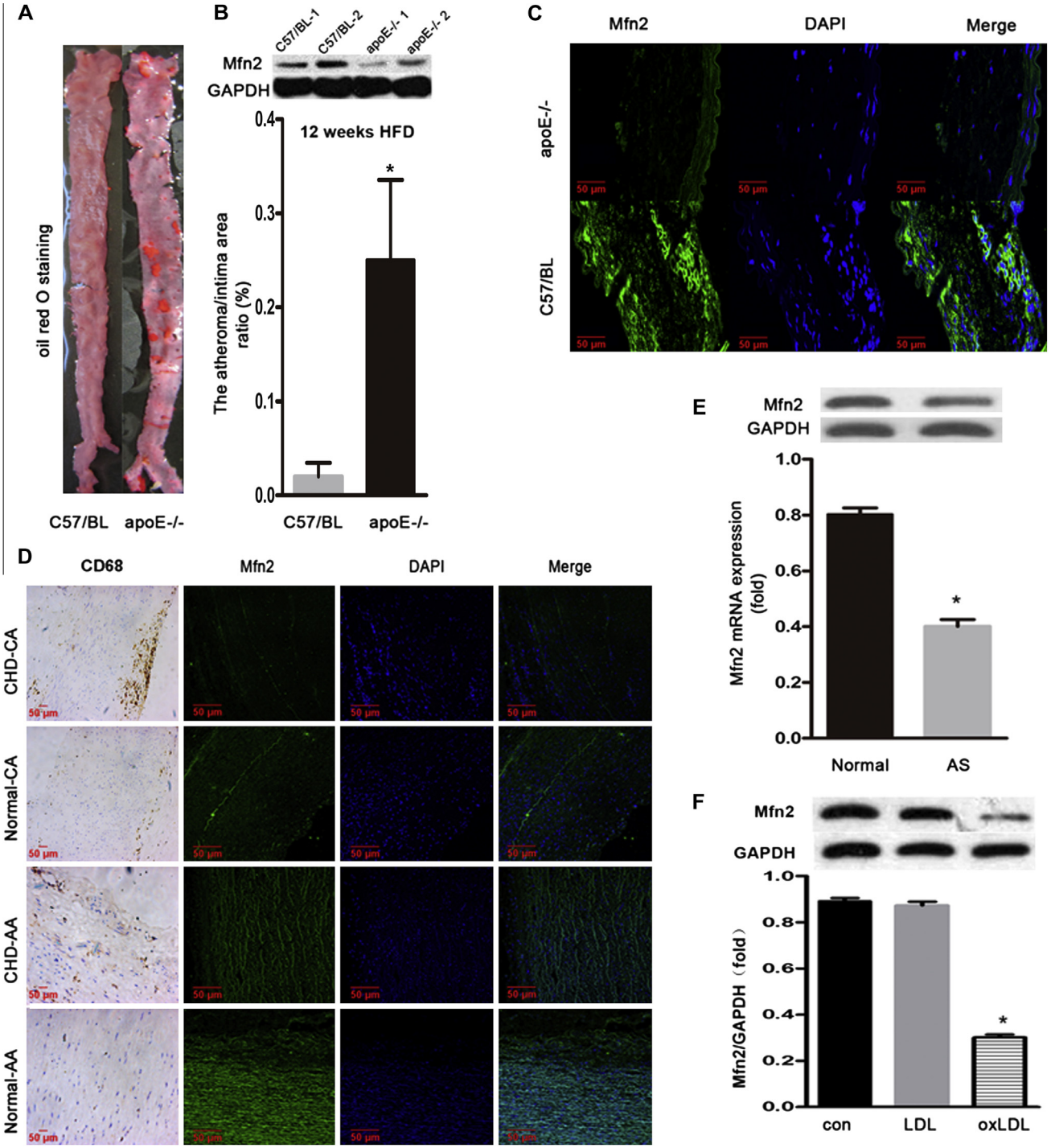

Fig. 1. Mfn2 expression in the atherosclerotic vascular of mice and humans and in macrophage-derived foam cells. The band intensity of Mfn2 was normalized to GAPDH. (A) Representative images of atherosclerotic lesions in aortas from apoE−/− or C57/BL mice, by en face staining with oil red O. (B) Western blot of Mfn2 in arteries of mice (apoE−/− and C57/BL) (above) and quantitative analysis of the atherosclerostic area by Image-Pro Plus software (below). Data are mean ± SD ($n = 6$); $^*p < 0.05$ vs. C57/BL. (C) Immunofluorescence for Mfn2 in arteries of apoE−/− and C57/BL mice. Green, Mfn2 in blood vessels; blue, nuclei stained with DAPI. Scale bars, 50 μm. (D) Immunofluorescence and immunohistochemistry for Mfn2 in atherosclerotic (CHD) and nonatherosclerotic (Normal) human arteries. Brown, CD68-positive macrophages; Green, Mfn2 in blood vessels; blue, nuclei stained with DAPI. Scale bars, 50 μm. (E) Western blot and real-time PCR of Mfn2 expression in human coronary arteries. Data are mean ± SD ($n = 6$); $^*p < 0.05$ vs. Normal. (F) Cell lysate extracted from macrophages treated with or without oxLDL (80 μg/mL, 24 h) for Mfn2 expression by Western blot analysis. Data are mean ± SD ($n = 4$); $^*p < 0.05$ vs. control. (For interpretation of the references to color in this figure legend, the reader is referred to the web version of this article.)

led to substantial increases in ABCA1, ABCG1 and SR-BI protein expression, while adv-siRNA mediated knockdown of Mfn2 abolished the induction, with attenuation by 39.3% for ABCA1, 68.3% for ABCG1, and 50.4% for SR-BI ($p < 0.05$; Fig. 2E). Similarly, we found that overexpression of Mfn2 led to increased PPARγ protein expression, while Mfn2 knockdown reduced PPARγ protein

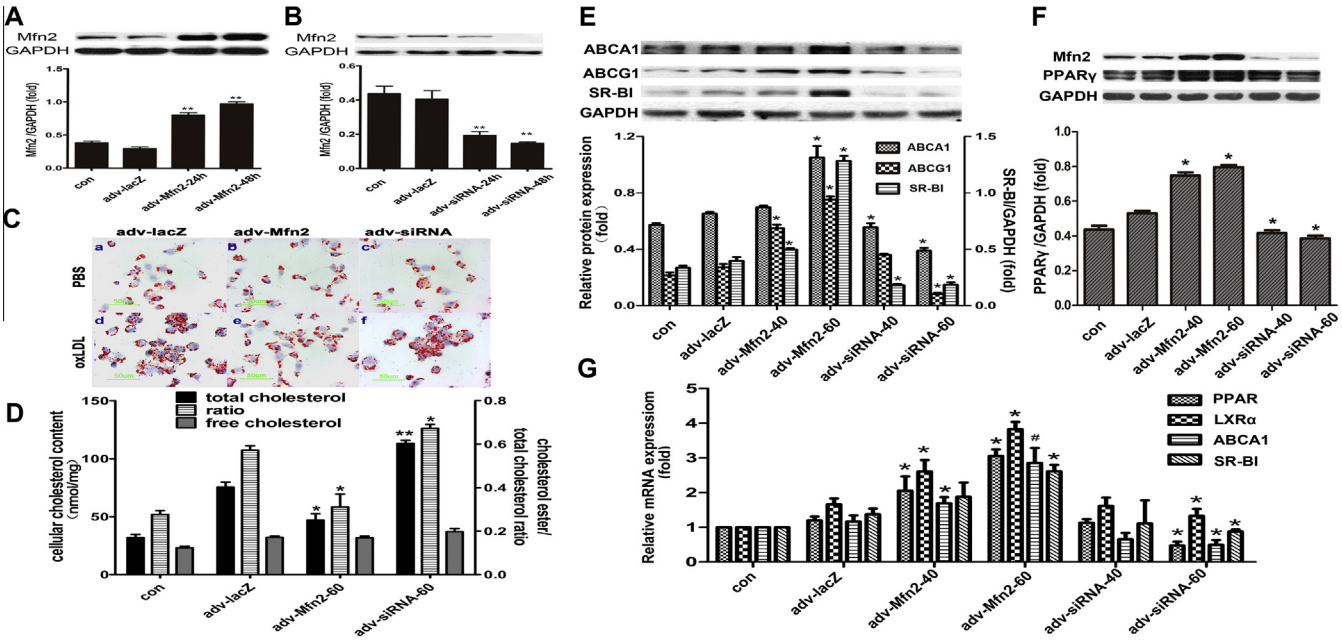

Fig. 2. Effect of Mfn2 on lipid accumulation and cholesterol transporter expression in macrophages. (A) and (B) After incubation with PBS, adv-lacZ for 48 h, or adv-Mfn2 and adv-siRNA for 24 or 48 h, the Mfn2 expression determined by western blot with GAPDH as a loading control. A representative blot from four separate experiments is shown. $^{**}p < 0.01$ vs. oxLDL plus adv-lacZ; (C) Oil red O staining in empty vector control (adv-lacZ, a and d), Mfn2-overexpressing cells (adv-Mfn2, b and e) and Mfn2-silencing cells (adv-siRNA, c and f), incubated in the presence (d, e and f) or absence (a, b and c) of oxLDL (80 μg/mL, 24 h) (magnification, ×400; scale bars, 50 μm); (D) The effect of Mfn2 on cellular cholesterol accumulation in THP-1 cells. Total and free cholesterol levels were determined after 24 h with oxLDL. Ratio of cholesterol ester to total cholesterol was plot on the right *Y* axis. Data are mean ± SD from three independent experiments. $^{**}p < 0.01$ versus oxLDL plus adv-lacZ. (E) Cells were incubated with or without indicated adenovirus for 24 h then PBS (control) or oxLDL (80 μg/mL) for 24 h. (E) ABCA1, ABCG1, SR-BI, (F) PPARγ protein by Western blot with GAPDH as loading control. A representative blot of three separate experiments is shown. (G) PPARγ, LXRα, ABCA1 and SR-BI mRNA by real-time PCR. Values are means ± SD, $n = 4$. Bars with a symbol are significantly different, $^{*}p < 0.05$ versus oxLDL plus adv-lacZ, $^{\#}p < 0.05$ versus adv-Mfn2-40.

expression (Fig. 2F). Besides, immune-fluorescence revealed no significant reduction in SR-A immunostaining in Mfn2-transduced macrophages (Supplemental Fig. S2).

Quantitative real-time PCR analysis showed that mRNA levels of PPARγ, LXRα, ABCA1 and SR-BI were significantly increased in adv-Mfn2 infected macrophages, but was significantly decreased in adv-siRNA infected cells, compared to controls ($p < 0.05$; Fig. 2G).

3.4. Mfn2 induces ABCA1, ABCG1 and SR-BI expression through PPARγ pathway

To clarify the role of PPARγ in Mfn2-induced anti-atherosclerotic effects, we examined the effects of PPARγ agonists and antagonists on Mfn2-mediated upregulation of cholesterol transport proteins. PPARγ antagonist GW9662 partially suppressed Mfn2-induced ABCA1, ABCG1 and SR-BI expression by 11.7%, 20% and 57.9%, respectively (Fig. 3A). However, overexpression of Mfn2 and PPARγ agonist rosiglitazone had an additive effect to increase ABCG1 expression (Fig. 3B). Furthermore, GW9662 strengthened adv-siRNA mediated suppression of SR-BI expression (Fig. 3C), while rosiglitazone abrogated adv-siRNA mediated suppression of ABCG1 and SR-BI expression (Fig. 3D).

Moreover, quantitative real-time PCR showed that adv-Mfn2 induced ABCA1 and ABCG1 transcription, which was suppressed by pretreatment with GW9662 (Fig. 3E). Adv-siRNA reduced baseline ABCA1 and ABCG1 transcription, and attenuated the stimulation of ABCA1 transcription by rosiglitazone (Fig. 3F). GW9662 alone could suppress ABCA1 and ABCG1 transcription, but no additive effect was observed by pretreatment with adv-siRNA (Fig. 3F). Taken together, these data suggest that PPARγ activation is involved in Mfn2-mediated upregulation of cholesterol transport proteins in macrophages.

3.5. Mfn2 induces PPARγ activation by inhibiting the activation of ERK1/2 and p38 in macrophages

To elucidate the mechanism by which Mfn2 promotes PPARγ activation, we focused on the MAPK pathway because Mfn2 was shown to inhibit ERK1/2 phosphorylation to regulate vascular smooth muscle cell proliferation [13]. Western blot analysis showed that the phosphorylation of ERK1/2 was dose-dependently inhibited in adv-Mfn2 infected THP-1 cells compared to adv-lacZ treated cells (Fig. 4A). Consistently, the phosphorylation of ERK1/2 was increased in adv-siRNA infected THP-1 cells, and this effect could be antagonized by pretreatment with ERK1/2 specific inhibitor PD98059 (Fig. 4B). Furthermore, adv-Mfn2 reduced the phosphorylation of p38 MAPK in THP-1 cells, and this effect was facilitated by pretreatment with p38 specific inhibitor SB203580 (Fig. 4C).

Next, we examined the regulation of ABCA1 and SR-BI expression by the MAPK pathway. Quantitative real time PCR analysis showed that mRNA expression of ABCA1 and SR-BI in macrophages was downregulated by adv-siRNA compared with vector control (adv-lacZ), but was upregulated by incubation with SB203580 or PD98059 (Fig. 4D). Furthermore, the upregulation of ABCA1 and (or) SR-BI by SB203580 or PD98059 could be partially abrogated by adv-siRNA (Fig. 4D). These results suggest that Mfn2 promotes while the MAPK pathway inhibits the expression of ABCA1 and SR-BI.

Accumulating evidence shows that the phosphorylation of Ser112 of PPARγ is mediated by ERK1/2, and PD98059 increased PPARγ activity in macrophages [4]. We found that adv-Mfn2 decreased while adv-siRNA increased PPARγ phosphorylation (Fig. 4E). Furthermore, Mfn2-induced suppression of PPARγ phosphorylation was promoted by treatment with p38 inhibitor

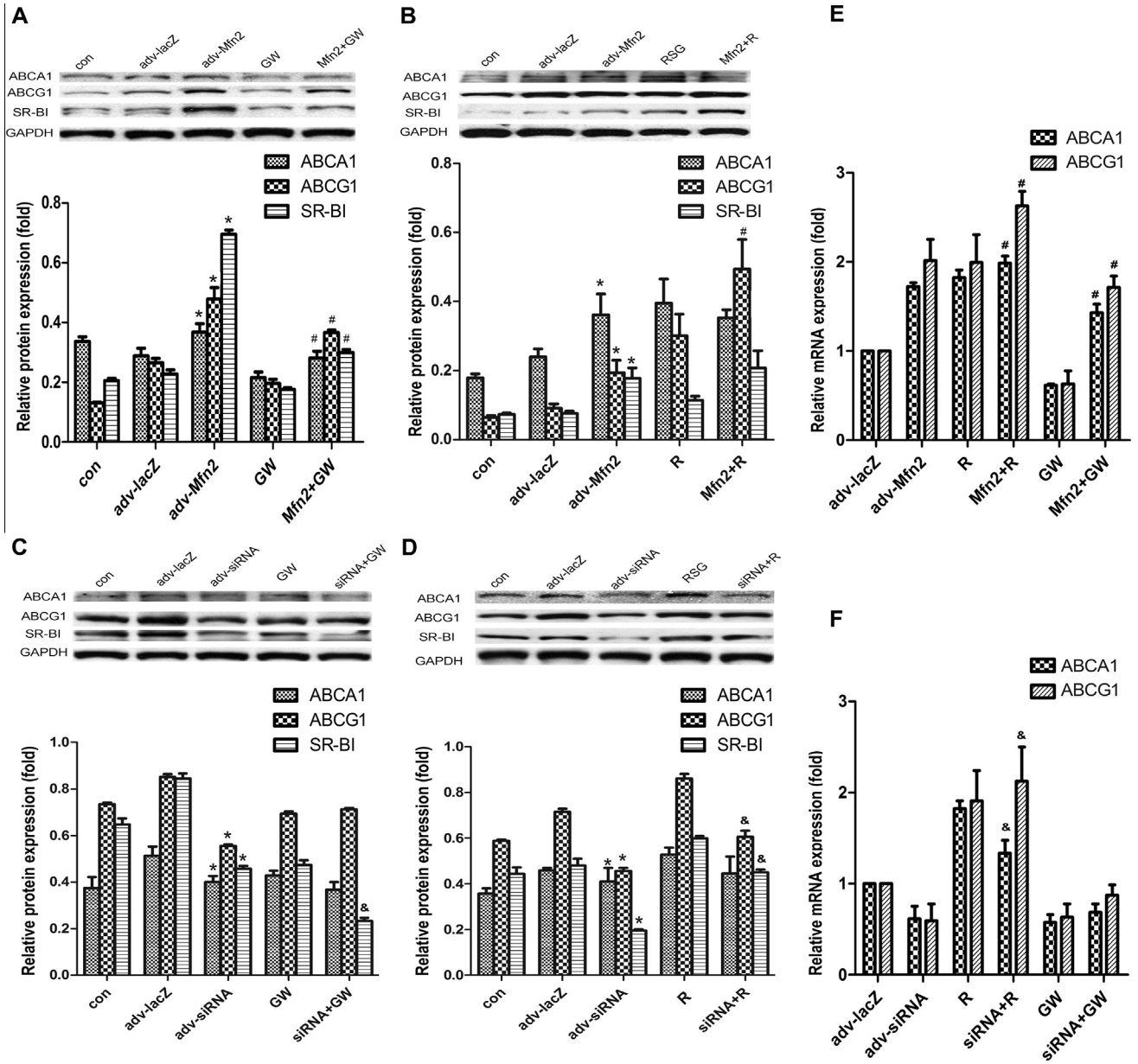

Fig. 3. Mfn2 and PPARγ agonists and antagonists and expression of cholesterol transporter in THP-1 macrophages. Cells were incubated with PBS, adv-lacZ, adv-Mfn2 or adv-siRNA for 24 h, and GW9662 (GW; 10 μM) or rosiglitazone (R; 10 μM) together with oxLDL were added for more 24 h. (A)–(D) Western blots. A representative blot of three separate experiments is shown and GAPDH was the loading control. Values are means ± SD. (E) and (F) real-time PCR. Values are means ± SD, $n = 4$. Bars with a symbol are significantly different. $^{*}p < 0.05$ compared with empty vector control (adv-lacZ /oxLDL). $^{\#}p < 0.05$ and $^{\&}p < 0.05$ compared with adv-Mfn2 and adv-siRNA, separately).

SB203580 or/and ERK inhibitor PD98059 (Fig. 4F). These results suggest that Mfn2 induces PPARγ activation by inhibiting the activation of ERK1/2 and p38 in macrophages.

4. Discussion

In the present study, we explored the potential atheroprotective actions of Mfn2 on cholesterol metabolism in foam cells. Our results showed that Mfn2 expression at both protein and mRNA levels was significantly reduced in arterial atherosclerotic lesion in both mice and human compared to that in healthy counterparts. Overexpression of Mfn2 alleviated cholesterol deposition in foam cells, accompanied by increased expression of ABCA1, ABCG1 and SR-BI, while Mfn2 knockdown led to opposite effects. Moreover, Mfn2 knockdown increased PPARγ phosphorylation and decreased PPARγ mRNA and protein levels. Lastly, we found that Mfn2 silencing decreased PPARγ-induced ABCA1, ABCG1 and SR-BI expression via inhibiting the activation of ERK1/2-MAPK and p38-MAPK pathways.

Mfn2, first named hyperplasia suppressor gene (HSG), mediates mitochondrial fusion and maintains mitochondrial morphology and function. Mitochondria have mostly been suggested to be related to atherosclerosis in three mechanisms [8]. Firstly, they are the major site of ROS generation, which causes the oxidation of LDL and cellular oxidative stress, contributing to the pathogenesis of atherosclerosis [14]. Secondly, mitochondrial cholesterol transport is considered to be a crucial hinge to control macrophage cholesterol efflux, the initial step of the regression and stabilization of atherosclerotic lesions [10,11]. In addition, mitochondrial dysfunction results in the accumulation of mitochondrial DNA damage and respiratory chain deficiencies, triggering signaling cascades for

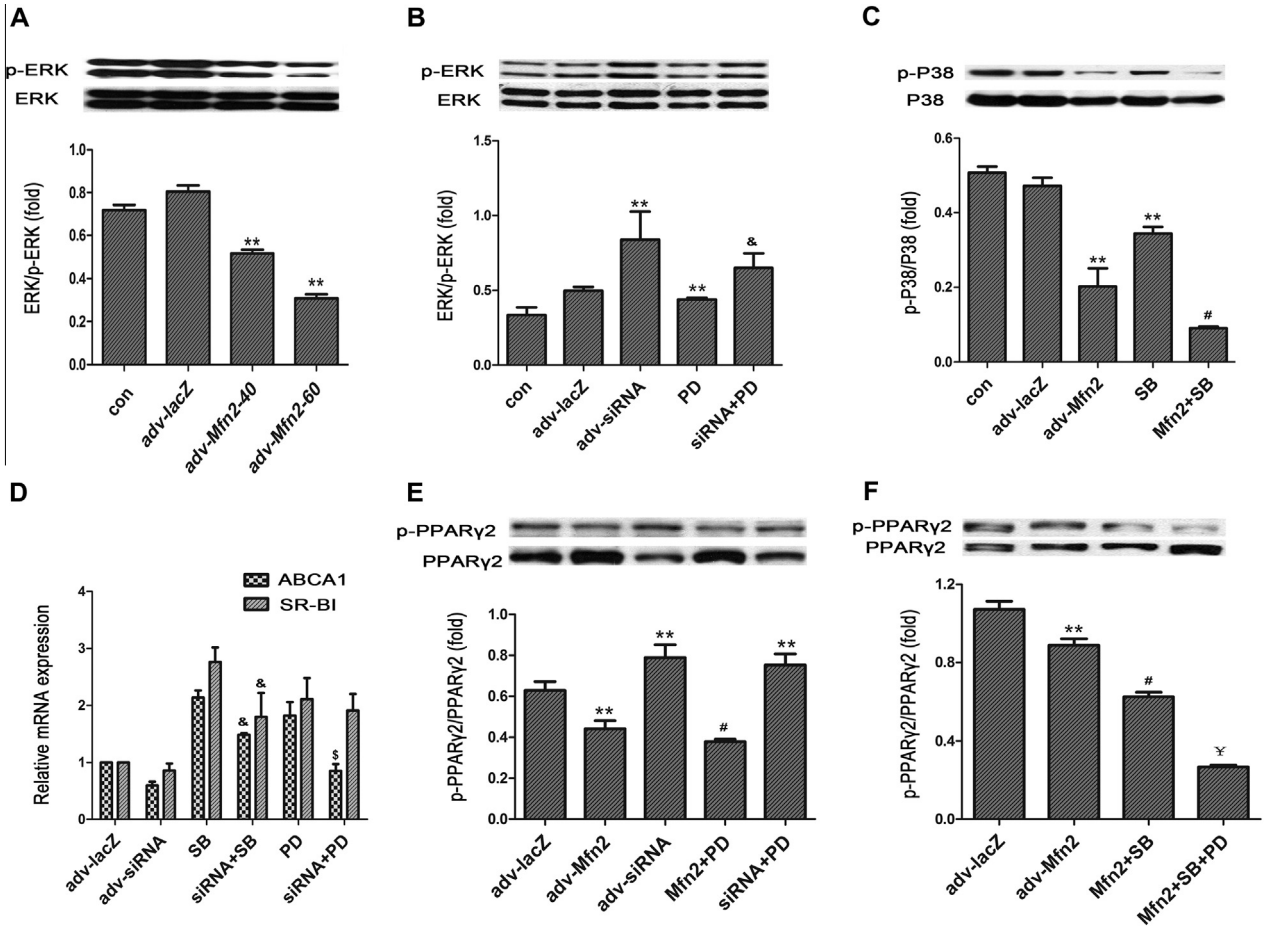

Fig. 4. Role of MAPK in Mfn2-induced PPARγ activation. Cells were incubated with PBS, adv-lacZ, adv-Mfn2 or adv-siRNA for 24 h in the absence or presence of PD98059 (PD; 10 μM) or SB203580 (SB; 10 μM). (A)–(C) After 24 h, expression of p-ERK1/2, ERK1/2, p-p38 and p38 protein was evaluated by Western blot. Data are means ± SD of three separate experiments. (D) After 24 h, expression of ABCA1, SR-BI or GAPDH mRNA was evaluated by real-time PCR. (E) and (F) After 24 h, samples were immunoblotted with anti-p-PPARγ2 or anti-PPARγ2 antibodies. Data are means ± SD of three separate experiments. Bars with a symbol are significantly different, $^{**}p < 0.01$ vs. adv-lacZ, $^{\#}p < 0.05$ vs. adv-Mfn2, $^{\&}p < 0.05$ vs. SB, $^{\$}p < 0.05$ vs. PD, $^{¥}p < 0.05$ vs. cells with adv-Mfn2 plus SB203580.

cell necrosis and apoptosis, endothelial cell dysfunction and impaired cholesterol efflux [15–17]. These events favor plaque formation and instability, culminating in the development of atherosclerosis.

However, very few studies have focused on the possible relationship between Mfn2 and atherosclerosis. Most research attention on Mfn2 has been devoted to its role in pathogenesis of vascular diseases, obesity, type 2 diabetes and diabetic nephropathy [13,16,18,19]. Only two animal studies passingly mentioned its relationship with atherosclerosis. One finds that overexpression of Mfn2 attenuated atherosclerotic lesion formation in rabbit carotid arteries by 66.7% and intima/media ratios by 74.6% due to its inhibition in proliferation of VSMCs, compared with that in control groups [18]. The other is one of our previous studies which reveals that Mfn2 expression was progressively reduced in carotid arteries of apoE−/− mice, along with atherosclerosis development [20]. In this study, we highlight the relationship between Mfn2 and atherosclerosis. We compared the Mfn2 expression level between non-atherosclerotic C57/BL mice and atherosclerotic apoE−/− mice of C57/BL background. More importantly, we included experiments on Mfn2 expression of non-atherosclerotic and atherosclerotic human arteries. While silencing of Mfn2 has been shown to increase lipid accumulation and cellular TG content in adipocytes [12], or overexpression of Mfn2 decreases lipid accumulation in VSMCs [21], it remains unclear whether Mfn2 has similar effects on THP-1 derived foam cells. We found that adv-Mfn2 infection, compared with adv-lacZ infection, decreased lipid accumulation in foam cells. Simultaneously, cell cholesteryl ester level and cholesteryl ester/total cholesterol ratio in adv-Mfn2 infected foam cells, compared to control cells, were decreased while free cholesterol content was not significantly different. These results suggest that Mfn2 could regulate lipid accumulation in macrophages and help explain how the mitochondria participate in cholesterol homeostasis in macrophages.

Atherosclerosis development and foam cell formation can be prevented by cholesterol efflux from macrophages, the initial step in RCT which delivers excess cholesterol and phospholipids from peripheral cells to the liver [22]. Cholesterol efflux is mediated by several potential cellular transporters such as ABCA1, ABCG1 and SR-BI, which help maintain cellular cholesterol homeostasis [2]. Disturbance of ABCA1 and ABCG1 function in macrophages, particularly in the arterial wall, might facilitate foam cell formation and atherogenesis, and trigger inflammation in atherosclerotic lesions [23]. SR-BI, a scavenger receptor highly expressed in organs of cholesterol metabolism and steroidogenesis, plays an anti-atherogenic role as a lipoprotein-selective receptor and lipid trader [23,24]. However, previous studies have not yet extended to the effects of Mfn2 on cholesterol transport in foam cell formation. In this study, we demonstrate a critical role of Mfn2 in regulating these cholesterol transporters. On the one hand, Mfn2 overexpression significantly increased the expression of ABCA1, ABCG1 and SR-BI in a dose-dependent manner. Conversely, on the other hand,

Mfn2 knockdown inhibited the expression of these cholesterol efflux proteins in macrophages. Our results further corroborate previous studies that mitochondrial dysfunction impairs efficiency of cholesterol efflux [10,11], indicating the possible mechanism by which Mfn2 regulates cholesterol metabolism in foam cells.

Atherosclerosis plaques, especially macrophage-derived foam cell formations, are closely associated with the activation of PPARγ, which facilitates the expression of multiple transporters, including ABCA1, ABCG1, SR-B1 [2,25,26]. For example, PPARγ activation has been reported to enhance cholesterol efflux and attenuate atherosclerosis by inducing ABCA1/ABCG1 expression in apoE-deficient mice [5,27]. Thus we speculate that PPARγ may be indispensible in Mfn2 induced ABCA1/ABCG1 expression. We found that Mfn2 induced expression of cholesterol transporters was abolished by PPARγ antagonist GW9662, while promoted by PPARγ agonist rosiglitazone, suggesting that PPARγ is involved in the Mfn2-mediated improvement of cholesterol efflux protein expression.

Since PPARγ contains a consensus MAPK site in the AF-1 domain, the phosphorylation of serine 82 (or 112 for PPARγ 2) suppresses PPARγ transactivation [4]. Moreover, suppression of ERK1/2 is involved in nifedipine-induced dephosphorylation of PPARγ, thereby inducing ABCA1 expression in macrophages [6]. Thus we evaluated the effects of Mfn2 on the MAPK pathway. In agreement with our early findings in rat VSMCs [13,20], data in this study showed that Mfn2 also decreased ERK1/2 and p38 phosphorylation in macrophages. More importantly, their inhibitors strengthened Mfn2-induced PPARγ dephosphorylation, a pathway of PPARγ activation. Thus, it can be speculated that Mfn2-induced PPARγ activation may be mediated by inhibiting the activation of MAPK/ERK1/2 and MAPK/p38 pathways.

Collectively, these findings provide insights into potential mechanisms of Mfn2-mediated alterations in cellular cholesterol transport, indicating the anti-atherogenetic effects of Mfn2.

5. Conflict of interest

None declared.

Acknowledgments

This work was supported by Grants from the National Natural Science Foundation of China (Nos. 30971244, 81270353 and 2010CHB00601) and the National Basic Research Program of China (973 Program, No. 2012CB518004). We also thank Dr. Luo Na of the University of Hong Kong for her insightful comments on the rhetorical structure of the discussion section.

Appendix A. Supplementary data

Supplementary data associated with this article can be found, in the online version, at http://dx.doi.org/10.1016/j.bbrc.2014.06.005.

References

[1] P.C. Choy, Y.L. Siow, D. Mymin, O. Karmin, Lipids and atherosclerosis, Biochem. Cell Biol. 82 (2004) 212–224.
[2] Z.S. Nagy, Z. Czimmerer, L. Nagy, Nuclear receptor mediated mechanisms of macrophage cholesterol metabolism, Mol. Cell. Endocrinol. 368 (2013) 85–98.
[3] C.M. Yang, Y.L. Lu, H.Y. Chen, M.L. Hu, Lycopene and the LXRalpha agonist T0901317 synergistically inhibit the proliferation of androgen-independent prostate cancer cells via the PPARgamma-LXRalpha-ABCA1 pathway, J. Nutr. Biochem. 23 (2012) 1155–1162.
[4] K.A. Burns, J.P. Vanden Heuvel, Modulation of PPAR activity via phosphorylation, Biochim. Biophys. Acta 1771 (2007) 952–960.
[5] F.A. Monsalve, R.D. Pyarasani, F. Delgado-Lopez, R. Moore-Carrasco, Peroxisome proliferator-activated receptor targets for the treatment of metabolic diseases, Mediators Inflamm. 2013 (2013) 549627.
[6] N. Ishii, T. Matsumura, H. Kinoshita, K. Fukuda, H. Motoshima, T. Senokuchi, S. Nakao, A. Tsutsumi, S. Kim-Mitsuyama, T. Kawada, M. Takeya, N. Miyamura, T. Nishikawa, E. Araki, Nifedipine induces peroxisome proliferator-activated receptor-gamma activation in macrophages and suppresses the progression of atherosclerosis in apolipoprotein E-deficient mice, Arterioscler. Thromb. Vasc. Biol. 30 (2010) 1598–1605.
[7] P. Dromparis, E.D. Michelakis, Mitochondria in vascular health and disease, Annu. Rev. Physiol. 75 (2013) 95–126.
[8] N.R. Madamanchi, M.S. Runge, Mitochondrial dysfunction in atherosclerosis, Circ. Res. 100 (2007) 460–473.
[9] D. Bach, D. Naon, S. Pich, F.X. Soriano, N. Vega, J. Rieusset, M. Laville, C. Guillet, Y. Boirie, H. Wallberg-Henriksson, Expression of Mfn2, the Charcot-Marie-Tooth neuropathy type 2A gene, in human skeletal muscle effects of type 2 diabetes, obesity, weight loss, and the regulatory role of tumor necrosis factor α and interleukin-6, Diabetes 54 (2005) 2685–2693.
[10] A.M. Allen, A. Graham, Mitochondrial function is involved in regulation of cholesterol efflux to apolipoprotein (apo)A-I from murine RAW 264.7 macrophages, Lipids Health Dis. 11 (2012) 169.
[11] A.M. Allen, J.M. Taylor, A. Graham, Mitochondrial (dys)function and regulation of macrophage cholesterol efflux, Clin. Sci. (Lond.) 124 (2013) 509–515.
[12] K.X. Gan, C. Wang, J.H. Chen, C.J. Zhu, G.Y. Song, Mitofusin-2 ameliorates high-fat diet-induced insulin resistance in liver of rats, World J. Gastroenterol. 19 (2013) 1572–1581.
[13] X. Guo, K.H. Chen, Y. Guo, H. Liao, J. Tang, R.P. Xiao, Mitofusin 2 triggers vascular smooth muscle cell apoptosis via mitochondrial death pathway, Circ. Res. 101 (2007) 1113–1122.
[14] S. Abhijit, R. Bhaskaran, A. Narayanasamy, A. Chakroborty, N. Manickam, M. Dixit, V. Mohan, M. Balasubramanyam, Hyperinsulinemia-induced vascular smooth muscle cell (VSMC) migration and proliferation is mediated by converging mechanisms of mitochondrial dysfunction and oxidative stress, Mol. Cell Biochem. 373 (2013) 95–105.
[15] S.B. Ong, D.J. Hausenloy, Mitochondrial morphology and cardiovascular disease, Cardiovasc. Res. 88 (2010) 16–29.
[16] Y. Chen, Y. Liu, G.W. Dorn 2nd, Mitochondrial fusion is essential for organelle function and cardiac homeostasis, Circ. Res. 109 (2011) 1327–1331.
[17] J. Li, X. Liu, H. Wang, W. Zhang, D.C. Chan, Y. Shi, Lysocardiolipin acyltransferase 1 (ALCAT1) controls mitochondrial DNA fidelity and biogenesis through modulation of MFN2 expression, Proc. Natl. Acad. Sci. U.S.A. 109 (2012) 6975–6980.
[18] Y.H. Guo, K. Chen, W. Gao, Q. Li, L. Chen, G.S. Wang, J. Tang, Overexpression of Mitofusin 2 inhibited oxidized low-density lipoprotein induced vascular smooth muscle cell proliferation and reduced atherosclerotic lesion formation in rabbit, Biochem. Biophys. Res. Commun. 363 (2007) 411–417.
[19] D. Sebastian, M.I. Hernandez-Alvarez, J. Segales, E. Sorianello, J.P. Munoz, D. Sala, A. Waget, M. Liesa, J.C. Paz, P. Gopalacharyulu, M. Oresic, S. Pich, R. Burcelin, M. Palacin, A. Zorzano, Mitofusin 2 (Mfn2) links mitochondrial and endoplasmic reticulum function with insulin signaling and is essential for normal glucose homeostasis, Proc. Natl. Acad. Sci. U.S.A. 109 (2012) 5523–5528.
[20] K.H. Chen, X. Guo, D. Ma, Y. Guo, Q. Li, D. Yang, P. Li, X. Qiu, S. Wen, R.P. Xiao, J. Tang, Dysregulation of HSG triggers vascular proliferative disorders, Nat. Cell Biol. 6 (2004) 872–883.
[21] C. He, Y. Chen, C. Liu, M. Cao, Y.J. Fan, X.M. Guo, Mitofusin2 decreases intracellular cholesterol of oxidized LDL-induced foam cells from rat vascular smooth muscle cells, J. Huazhong Univ. Sci. Technolog. Med. Sci. 33 (2013) 212–218.
[22] I. Voloshyna, A.B. Reiss, The ABC transporters in lipid flux and atherosclerosis, Prog. Lipid Res. 50 (2011) 213–224.
[23] A. Dikkers, J. Freak de Boer, W. Annema, A.K. Groen, U.J. Tietge, Scavenger receptor BI and ABCG5/G8 differentially impact biliary sterol secretion and reverse cholesterol transport in mice, Hepatology 58 (2013) 293–303.
[24] S. Saddar, V. Carriere, W.R. Lee, K. Tanigaki, I.S. Yuhanna, S. Parathath, E. Morel, M. Warrier, J.K. Sawyer, R.D. Gerard, R.E. Temel, J.M. Brown, M. Connelly, C. Mineo, P.W. Shaul, Scavenger receptor class B type I is a plasma membrane cholesterol sensor, Circ. Res. 112 (2013) 140–151.
[25] Z.S. Nagy, Z. Czimmerer, L. Nagy, Nuclear receptor mediated mechanisms of macrophage cholesterol metabolism, Mol. Cell Endocrinol. 368 (2013) 85–98.
[26] A. Szanto, T. Roszer, Nuclear receptors in macrophages: a link between metabolism and inflammation, FEBS Lett. 582 (2008) 106–116.
[27] H. Ozasa, M. Ayaori, M. Iizuka, Y. Terao, H. Uto-Kondo, E. Yakushiji, S. Takiguchi, K. Nakaya, T. Hisada, Y. Uehara, M. Ogura, M. Sasaki, T. Komatsu, S. Horii, S. Mochizuki, M. Yoshimura, K. Ikewaki, Pioglitazone enhances cholesterol efflux from macrophages by increasing ABCA1/ABCG1 expressions via PPARgamma/LXRalpha pathway: findings from in vitro and ex vivo studies, Atherosclerosis 219 (2011) 141–150.